Long-lived photoinduced response observed under extreme photoexcitation densities in a one-dimensional Peierls insulator

Johanna W. Wolfson,[1] Samuel W. Teitelbaum,[1] Taeho Shin,[2] Ikufumi Katayama,[3] Taro Kawano,[3] Jun Takeda,[3] and Keith A. Nelson[1,*]

[1]*Department of Chemistry, Massachusetts Institute of Technology, Cambridge, Massachusetts 02139, USA*
[2]*Department of Chemistry, Chonbuk National University, Jeonju 54896, Republic of Korea*
[3]*Graduate School of Engineering, Yokohama National University, Yokohama 240-8501, Japan*

One-dimensional metal-halide compounds provide model systems to investigate the manner in which coupling between elementary degrees of freedom—here, electronic and vibrational—result in instabilities that give rise to both chemical and structural rearrangements. Here, we employ "single-shot" pump-probe spectroscopy to examine a one-dimensional platinum iodide compound (PtI(en)) under far-from-equilibrium conditions where repeated photoexcitation results in sample damage. It presents evidence for a distinct collective excited state lasting more than 100 ps upon self-trapped exciton generation at high densities, as measured by electronic signal amplitudes and phonon properties.

I. INTRODUCTION

Quasi-one-dimensional systems offer a unique view into the physics of electron-phonon coupling that leads to photoinduced structural phase transitions. Many quasi-one-dimensional systems form charge-ordered or charge density wave (CDW) states that are sensitive to photoexcitation [1]. Unlike their two-dimensional [2] and three-dimensional [3,4] counterparts, exciton self-trapping is always barrierless in one-dimensional systems [5]. In addition, the reduced dimensionality simplifies the physics, making the system close to the simplified model of a charge-ordering structural phase transition first proposed by Peierls [6].

Photoinduced dynamics in crystalline metal-halide chain compounds have stimulated decades of interest due to their straightforward structure yet complex interplay between electronic and vibrational degrees of freedom and between chemical and structural rearrangements [7–10]. One of these compounds, $[Pt(en)_2][Pt(en)_2I_2](ClO_2)_2$ [hereafter PtI(en)], is formed around one-dimensional (1D) chains of alternating Pt and I atoms [simplified structure shown in Fig. 1(a)]. Laser-induced electron transfer along the 1D chain axis launches coherent vibration of the halide ions along the same axis, creating a well-defined system that highlights the interplay among optical, electronic, and vibrational energies and their roles in local crystalline chemistry and collective, long-range lattice structure.

In PtI(en), the Coulomb repulsion energy is weak compared with electron-phonon interactions. The result is a lattice distortion into a structure with reduced symmetry, which produces a Peierls band gap that minimizes the electronic energy [6], analogous to the Jahn-Teller effect in isolated molecules. In the ground state, Pt centers exhibit alternate valences of $3 - \delta$ and $3 + \delta$, and Pt-I bond lengths alternate as

well (with a length ratio of 0.92 from one Pt-I bond to the next) [14]. The symmetric I-Pt(III $+ \delta$)-I stretch is Raman active and shows strong resonance enhancement and vibronic coupling near the charge-transfer transition [7,12], which has an onset at 1 eV and a peak at 1.3 eV [15]. Photoexcitation from the ground-state Peierls-distorted geometry into a charge-transfer exciton state initiates a large excursion along the symmetric stretch coordinate to form a self-trapped exciton (STE) species with locally equivalent Pt(III) ions. The transitions from charge density wave to free exciton to trapped exciton are illustrated in Fig. 1(b), which shows the highly localized two-site limit. A more detailed theory predicts that the STE is delocalized over more than 20 unit cells in PtI(en) [13,16].

PtI(en) lattice vibrations associated with STE formation around 125 cm^{-1} have been reported from time-domain studies [10,17,18], corresponding to the ground-state symmetric stretch in the resonant Raman spectrum [12]. In addition, wave-packet motion at 106 cm^{-1} along the fully formed STE state has been resolved in the time-domain spectrum of photoexcited PtI(en) [19]. The STE lifetime in Pt-halide chain complexes has been reported to be on the order of 5 ps, as determined by the signal decay time after STE formation [20]. Once the self-trapped exciton is formed, it can decay into a variety of electron-lattice coupled quasiparticles, such as solitons and free polarons [13,21]. All the electronically excited states have reduced Peierls distortions and Pt charge alternations relative to the ground state [16]. Completely equivalent Pt(III) ions and equal Pt-I bond lengths would result in a Raman-inactive symmetric stretching mode, and the approach of the system toward the high-symmetry state is expected to lead to suppression of pump-probe excited oscillation amplitude of this vibrational mode.

Though conventional time-resolved pump-probe spectroscopy has provided descriptions of STE formation in PtI(en) and related materials [8,10,22–25], the technique's investigative utility is restricted to reversible material changes due to
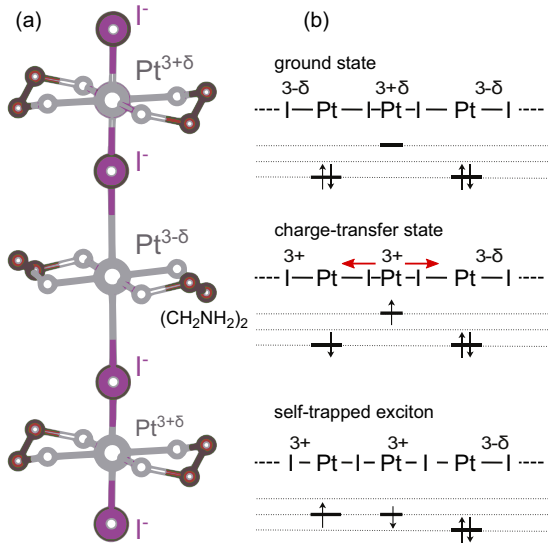
*kanelson@mit.edu

FIG. 1. (a) Simplified schematic illustration of the crystal structure of $[PtI(en)_2]_2(ClO_4)_4$. Pt and I atoms are arranged in 1D chains with alternating Pt^{2+} and Pt^{4+} ions and alternating Pt-I bond lengths (exaggerated). Perchlorate counterions (not shown) neutralize the net-positive charge of the 1D chains. (b) Schematic illustration of the formation of a self-trapped exciton (STE) in PtI(en), as viewed along the PtI chains. In the highly localized (small polaron) limit, a charge-transfer transition generates a pair of Pt^{3+} ions, exciting a Raman-active vibration along the chain axis and equalizing Pt-I bond lengths. This is a simplified picture, and it is predicted that the STE is delocalized over several unit cells, and the charge separation is a fraction of an electron [$\delta = 0.36\ e^-$ in PtI(en)] [11]. Figure adapted from [12,13].

FIG. 2. (a) Reversible pump-probe traces of PtI(en) at low fluence (from 0.2 to 1.6 mJ/cm^2). The pump and probe wavelengths are both 800 nm. (b) Fluence dependence of the reflectivity change at $t = 0$ of the traces shown in (a) (blue points). The dashed line shows an exponential fit to the fluence dependence.

the thousands of repeated pump-probe sequences required. We have adopted a method that enables the complete time-dependent response to photoexcitation to be measured with good signal to noise with only 100 laser shots, reporting in real time as the system undergoes irreversible change [26,27].

In this work we first characterize PtI(en) responses to moderate pump pulse fluences with conventional techniques and demonstrate that sample damage precludes conventional measurements at high pump fluences. We then present results from single- and double-pump measurements using the single-shot spectroscopy, the latter in which a second pump pulse excites the lattice after exciton states have already been produced by a first pump pulse. Measurements above 4.5 mJ/cm^2 pump fluence demonstrate evidence of a collective excited state with a lifetime greater than 100 ps. This state reflects underlying structural rearrangements toward a higher-symmetry phase and is revealed through electronic and vibrational properties of the photoexcited lattice measured at varying time delays up to 100 ps after STE formation. This long-lived excited state is only observed at excitation densities above the cumulative damage threshold, requiring single-shot methods to observe it.

II. METHODS AND RESULTS

The laser system used for both conventional and single-shot measurements consists of a mode-locked Ti:sapphire laser and a 1-kHz repetition rate regenerative amplifier that
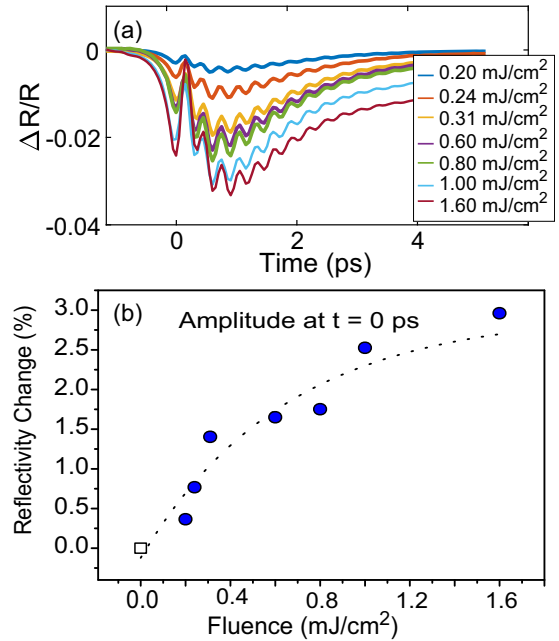
generates 800-nm pulses with energies of 2.5–3.0 mJ/pulse. The conventional pump-probe measurements were conducted with a lock-in amplifier and a mechanical chopper operated at 500-Hz repetition rate. For single-shot measurements, a single pulse selector was operated at 10-Hz repetition rate and a mechanical shutter was used to select individual pulses. A wavelength of 800 nm was used for both the pump and probe beams in the conventional pump-probe measurements. On the other hand, a 600-nm wavelength generated from a noncollinear optical parametric amplifier (NOPA) was used for probe pulses with an 800-nm pump pulse for the single-shot pump probe measurements because it prevents the pump beam from scattering into the CCD camera with a band-pass filter. The pump photon energy of 1.55 eV (800 nm) was well above the charge-transfer transition energy of 1 eV for PtI(en). The pump and probe polarizations were parallel to the 1D chain axis of the crystal.

The samples are single crystals of PtI(en) and were synthesized from perchloric acid ($HClO_4$) solutions of the complexes $[Pt(en)_2I_2]I_2$ and $[Pt(en)_2](ClO_4)_2$ [28,29], and were recrystallized from water solution grown by a similar method to those in previous work [28,29].

Figure 2(a) shows time-dependent differential reflectivity data from PtI(en) recorded using conventional pump-probe methods. Responses following 800-nm pump pulses with fluences between 0.20 and 1.6 mJ/cm^2 were probed by weak 800-nm probe pulses. The data show a reduction in reflectivity following pumping, and an oscillatory component at 120 cm^{-1} with a dephasing time of 3 ps, indicating relaxation of the initially excited state to the STE state. Though the STE lifetime has previously been reported to be 5 ps [20], which agrees with
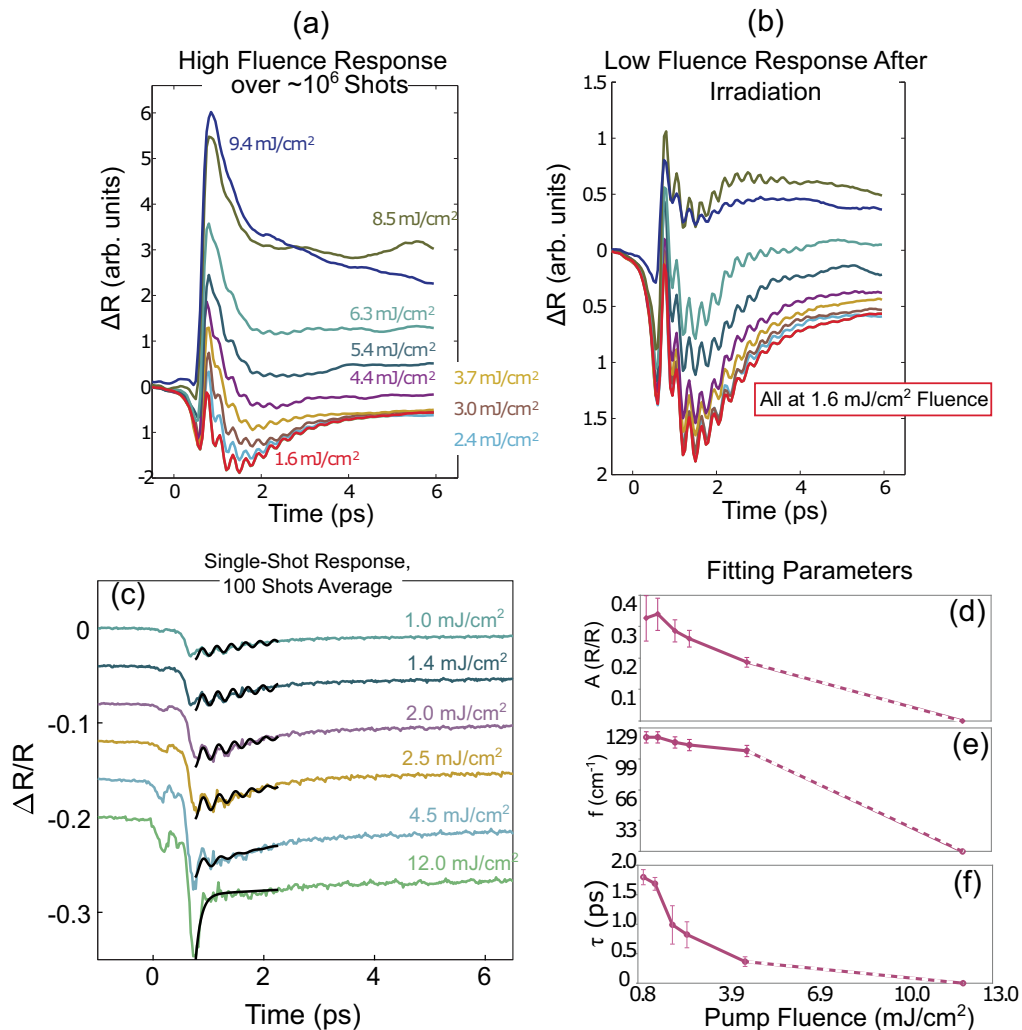
FIG. 3. (a) Reflectivity changes at various pump fluences obtained conventional pump-probe measurements with over 10^6 shots. (b) After preirradiation with pump fluence used in (a), reflectivity changes were obtained at the same spots under low pump fluence of 1.6 mJ/cm^2. The same colors of curves in (a) and (b) indicate the same spots for both measurements. For preirradiation above 2.4 mJ/cm^2 with over 10^6 shots, the sample shows irreversible damage, demonstrating the need for single-shot measurements. (c) Single-shot pump-probe data at various pump fluences below and above the damage threshold. The small feature before $t = 0$ is due to a prepulse in the amplifier. (d)–(f) Fit parameters showing fluence dependence of phonon properties, the oscillation amplitude relative to the total reflectivity change at $t = 0$ (d), oscillation frequency (e), and oscillation dephasing time (f) of the coherent phonon oscillation. The coherent phonon signal disappears at 12 mJ/cm^2. The error bars in (d)–(f) represent the uncertainty from the fitting analysis.

our results at low excitation density, we see clear evidence of a longer-lived response in the nonoscillatory component at higher pump fluences.

The reflectivity changes at $t = 0$ as a function of fluence are shown in Fig. 2(b). They seem linear with increasing fluence at low fluence below 0.6 mJ/cm^2 but increase sublinearly with increasing fluence. Although fluctuations in the reflectivity are large near zero fluence because of the uncertainty of the fluence measurements, they could be approximately fitted with an exponential function assuming a zero reflectivity change at zero fluence. The dotted line shows the fit in Fig. 2(b), and it has a characteristic fluence of 0.6 mJ/cm^2. It is estimated that the average size of a lattice deformation (self-trapped exciton) due to a single photoexcitation in PtI(en) is approximately 20 unit cells [18]. In order to convert fluence to absorbed photon density per site along the chain, we divide the absorbed energy

density by the Pt density

$$n_{Ph/Pt} = \frac{(1 - R)Fv}{4\delta E_p},$$ (1)

where R is the reflectivity (0.72), F is the incident fluence, v is the unit-cell volume (1.46 nm^3), E_p is the photon energy (1.55 eV), and δ is the optical penetration depth (110 nm). The factor of 4 is due to the four Pt atoms per unit cell. The characteristic fluence of 0.6 mJ/cm^2 corresponds to 0.045 photons per Pt ion.

The response of PtI(en) at higher fluences (2.4–9.4 mJ/cm^2) is shown in Fig. 3(a). The material response reveals drastically different time-dependent profiles. However, the observed responses were shown to result from cumulative degradation of the sample over many thousands of shots. We performed low-fluence measurements on individual sample regions after

they had been irradiated under high fluence. The results, shown in Fig. 3(b), differ markedly from the low-fluence response without prior high-fluence excitation, shown in Fig. 2(a), and from the high-fluence results in Fig. 3(a). We conclude that cumulative damage occurs above 2.4 mJ/cm^2, rendering conventional pump-probe measurements above this threshold unreliable. As elaborated below, the 2.4-mJ/cm^2 threshold corresponds to approximately 0.15 absorbed photons per Pt atom.

Even though the crystal undergoes irreversible damage at high fluence, it is worth seeing behaviors of oscillatory signal with increasing fluence in Fig. 3(a). The oscillations decrease with increasing fluence and become almost negligible at 8.5 and 9.4 mJ/cm^2. The disappearance of oscillations can be due to simple crystal damage or due to the material's true dynamic response. However, as seen in Fig. 3(b), it is obvious that the background signal changes irreversibly after damage due to preirradiation, but the strong oscillatory signal still exists and does not change almost at all, regardless of preirradiation fluence. This strongly implies that the oscillatory signal itself in Fig. 3(a) is close to true photo responses of PtI(en) and that the disappearance of oscillations is also a true materials response under high fluence. On the contrary, it is likely that the positively growing background signal with increasing fluence is due to an irreversible change of the damaged PtI(en) crystal, such as irreversible photobleaching.

We are interested in the material's true response to a single pulse rather than to the cumulative result of many pulses; however, averaging of data from multiple shots significantly improves signal-to-noise levels. The single-shot data presented here were collected and averaged over 100 laser shots whose separations were long enough to ensure full relaxation to the ground state. In each case, cumulative degradation was monitored by ensuring that low-fluence measurements yielded the same responses before and after the high-power shots, in the same manner as shown in Fig. 3(b). Although cumulative damage occurred after many shots, damage did not occur catastrophically after a single shot or after 100 shots. Each of the 100 shots was a true single-shot measurement, generating the full time window of data in response to one excitation event.

To examine the real-time photoinduced dynamics of PtI(en) above this threshold, we employed single-shot measurements for a range of pump fluences between 1.0 and 12 mJ/cm^2 using 800-nm pump and 600-nm probe wavelengths. Each single-shot measurement is conducted by overlapping the pump pulse at the sample with 400 probe pulses that were separated temporally by 22.6 fs to span a total temporal range of 9 ps. The reflected probe pulses reach different regions of a CCD detector so that the sample reflectivity at each of the 400 pump-probe delay times can be determined. More details of this method are described in our previous work [27]. We observed significant changes in reflectivity and in phonon behavior over this range, as shown in Fig. 3(c). At low fluences (1.0–1.4 mJ/cm^2), the familiar lattice vibrational response associated with STE formation was clearly observed. However, it appears that the dephasing times in single-shot pump-probe data in Fig. 3(c) are shorter compared to those from conventional pump-probe experiments in Fig. 2(a) and Fig. 3(a). This is because of the probe-wavelength dependence of the dephasing times. Sugita *et al.* investigated the wave-packet dynamics using reflectivity

measurements with a 5-fs time resolution and obtained the dephasing times as a function of probe wavelength [23]. The dephasing time of the wave packet decreases with probe wavelength from 1.77 to 2.00 eV when probed in reflection mode. This is attributed to vibrational relaxation of the wave packet on the self-trapped potential energy surface and relevant photoinduced absorption. Their observation is consistent with our results in which the dephasing time is shorter with a 600 nm probe wavelength than with an 800 nm probe wavelength. Besides the dependence on wavelength, single-shot measurements can yield shorter apparent dephasing times compared to those from ordinary pump-probe measurements due to lower signal-to-noise levels. As the fluence was increased up to 4.5 mJ/cm^2, we continued to observe coherent vibrational oscillations but with decreasing amplitude relative to the peak electronic signal level, frequency, and dephasing time as shown in Figs. 3(d)–3(f).

To fit the reflectivity traces after $t = 1$ ps, they were assumed to be a sum of two exponential decays (electronic background signal) and an exponentially decaying cosine function (oscillatory signal). The fitting parameters in Figs. 3(d)–3(f) and Figs. 4(b)–4(e) were obtained by first performing a least-squares fit of the traces after $t = 1$ ps to a sum of the two exponential decays (electronic background signal). This fit was then subtracted from the data to obtain the oscillatory part of the transient reflectivity change. The oscillatory part of the trace where the oscillations are present (from $t = 0$ to $t = 1.75$ ps) was then Fourier transformed to yield approximate Lorentzian functions. The frequency and dephasing time were then extracted from the frequency-domain fitting by the peak value and central frequency and FWHM of the Fourier transform. The oscillation amplitude was extracted from the first cycle in the subtracted signal. In this way, all of the parameters were obtained and then the reflectivity could be reconstructed. Final representative fits to single-shot traces are shown as black lines in Fig. 3(c).

At still higher pump fluence (12 mJ/cm^2), no coherent vibrational oscillations were observed in the data. The absence of observed oscillations at 12 mJ/cm^2 pump fluence could suggest rearrangement to a higher-symmetry state in the pumped region. Coherent oscillations are observed ordinarily because upon photoexcitation, the I ions are oscillating between their initial locations, which are closer to Pt$^{III+\delta}$ than to Pt$^{III-\delta}$, and their excited-state potential energy minima, which are closer to equidistant between Pt ions. In the symmetric state, vibrations in which I ions move about equilibrium positions that are equidistant between truly equivalent Pt^{III} ions are Raman inactive, since motion of the ions in either direction about those positions changes the optical properties of the crystal change in the same way so that $(\frac{dn}{dQ})_{sym} = 0$, where n is any component of the refractive index tensor and Q is the symmetric vibrational coordinate.

It is also possible that the absence of oscillations following high-fluence excitation might be due to dephasing; Fig. 3(f) shows that the dephasing time decreases as the fluence is increased. To address this ambiguity and investigate the lattice structure after strong pump excitation, we performed double-pump measurements with a second pump pulse that acted on the photoexcited state produced by the first pulse. A low
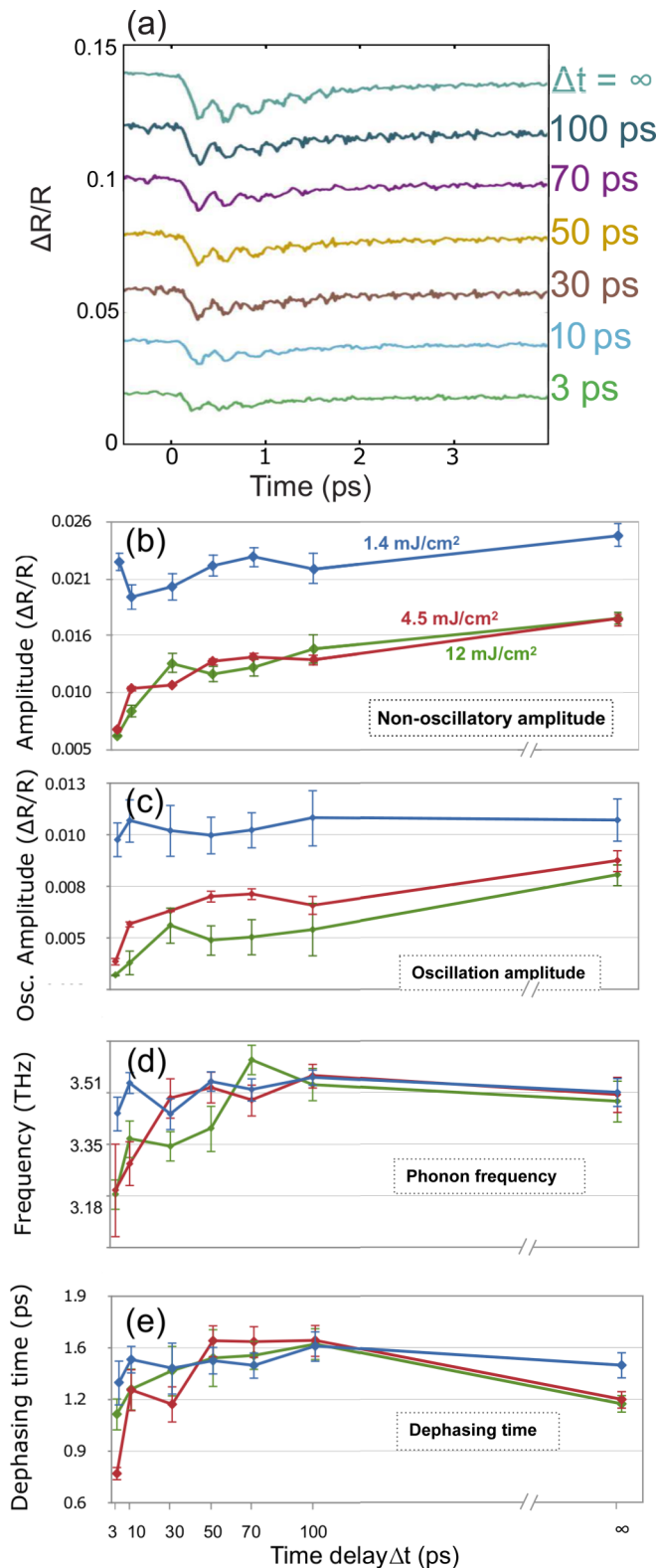
FIG. 4. Double-pump experiments performed with a 0.8-mJ/cm² second pump pulse reveal dynamics of the highly excited state. (a) Double-pump response with an initial excitation fluence of 12 mJ/cm² at various interpump delays. (b)–(e) Show fit parameters for the pump-probe response to the second pump as a function of interpump delay for 1.4, 4.5, and 12 mJ/cm² first-pulse fluence. The parameters shown are the nonoscillatory amplitude (b), the oscillation amplitude (c), the oscillation frequency (d), and the dephasing time (e). Infinite time

fluence of the second pump pulse (0.8 mJ/cm²) ensured that the second pulse itself did not drive the lattice far from equilibrium, but the time-dependent response—observed with 400 probe pulses overlapped with the weak second pump pulse—depended on the fluence of the first pump pulse and the time delay Δt between it and the second pump. For three fluences of the first pump pulse (1.4, 4.5, and 12 mJ/cm²), we pumped the lattice a second time Δt after the first pump, for a Δt of 0, 3, 10, 30, 50, 70, and 100 ps, as well as several seconds (effectively infinite time).

Results with a first-pulse fluence of 12 mJ/cm² are shown in Fig. 4(a). After the first pump pulse, the 0.8 mJ/cm² second pump pulse induces a response that reports on the state of the system at the time of arrival of the second pump pulse. The amplitude of oscillatory signals is clearly suppressed at short delay times Δt following the 12-mJ/cm² pump pulse; however, it never reaches zero amplitude, indicating that there is no full transformation to a higher-symmetry phase. It recovers substantially but not completely after 100 ps. The oscillation frequency and dephasing rate return to their unperturbed values (within somewhat large uncertainties) in under 100 ps. The observation of substantially reduced phonon signal amplitude at short delays suggests that the complete suppression of signal oscillations in single-pump data at 12 mJ/cm² fluence [shown in Fig. 3(c)] is due to a combination of collective structural changes and a fast dephasing rate.

The same fitting analysis as for Fig. 3(c) was performed to extract the fitting parameters of double-pump data with three different first-pump fluences. The results are summarized in Figs. 4(b)–4(e). The measured lattice properties (oscillation amplitude, phonon frequency, and dephasing time) remain relatively unchanged from Δt of 3 ps through Δt of 100 ps after the 1.4-mJ/cm² pump pulse. The electronic amplitude increases slightly over the Δt range, indicating the system takes more than 100 ps to relax back to equilibrium, even after moderate excitation fluence (well below the damage threshold). The excited lattice created by the 4.5-mJ/cm² pump pulse (Fig. 4) is clearly distinct from the STE state generated from the 1.4-mJ/cm² pulse, since both the short-time dynamics and the long-time electronic state differ between the two photoexcitation fluences. We postulate that this change is due to the high density of excitations generated at high fluence, which may result in correlated regions of altered lattice structure (e.g., polaronic quasiparticles) in which the reflectivity at the probe wavelength is reduced and in which the phonon properties are changed. As shown in Figs. 4(b) and 4(c), after the 4.5-mJ/cm² pump pulse, the oscillatory and nonoscillatory signals induced by the second pulse are less than half their amplitudes 3 ps after the arrival of the 1.4-mJ/cm² pump pulse. Similarly, the phonon frequency is reduced to 106 cm^{-1} [Fig. 4(d)], and the phonon dephasing time [Fig. 4(e)] is reduced to 0.8 ps for a time delay $\Delta t = 0.3$ ps. The excited lattice relaxes toward a final state that is not fully returned to the initial state after 100 ps, as shown by the continued suppression of the oscillatory signal amplitude. In contrast, the phonon frequency

corresponds to a measurement taken long after the second pump, approximately 1 min later. The error bars in (b)–(e) represent the uncertainty generated from the fitting analysis.

and dephasing time return to close to their equilibrium values within 50 ps after high-fluence excitation. This indicates that the long-lived state at high fluence is not a high density of self-trapped excitons but a collective excited state born out of the decay of a high density of self-trapped excitons.

Finally, the results of a first pump fluence of 12 mJ/cm^2 show all the same trends, with a somewhat greater reduction in the oscillatory signal amplitude, down to less than one-third of the original oscillatory signal. In addition, above the 4.5-mJ/cm^2 threshold, the coherent oscillation frequency shifts from 116 to 103 cm^{-1}. This is a much larger redshift than that at low excitation density, shown in Fig. 3(d). The reduced frequency is consistent with the 106-cm^{-1} frequency reported for the STE wave packet [11] and suggests that there has been a shift in the electronic and lattice structure such that the majority of the system is in the STE state for at least 10 ps. The high STE density results in further relaxation into long-lived quasiparticles with continued phonon signal suppression for over 100 ps. Two-pulse single-shot measurements reveal the suppression of the self-trapped exciton oscillation amplitude and electronic pump-probe signal for hundreds of picoseconds following photoexcitation above 4.5 mJ/cm^2, indicating the existence of a long-lived excited state not present at low excitation densities. This excited state is the result of the decay of a high density of self-trapped excitons and has a suppressed lattice distortion relative to the ground state.

III. CONCLUSIONS

We have measured electronic excited-state and coherent phonon dynamics in highly excited PtI(en). Strongly reduced lattice vibrational signals at excitation fluences above 4 mJ/cm^2 atom indicate shifts in the lattice structure toward a high-symmetry configuration with equal Pt-I bond lengths and monovalency of Pt ions. Long-lived electronic excitations reveal significant changes in the collective electronic structure at high excitation densities. Far-from-equilibrium dynamics in many systems with strong vibronic coupling, in which large changes in lattice structure upon strong excitation may be expected, can be examined directly with the single-shot femtosecond spectroscopy approach that we used.

[1] T. Huber, S. O. Mariager, A. Ferrer, H. Schäfer, J. A. Johnson, S. Grübel, A. Lübcke, L. Huber, T. Kubacka, C. Dornes, C. Laulhe, S. Ravy, G. Ingold, P. Beaud, J. Demsar, and S. L. Johnson, Phys. Rev. Lett. **113**, 026401 (2014).

[2] F. Schmitt, P. S. Kirchmann, U. Bovensiepen, R. G. Moore, L. Rettig, M. Krenz, J.-H. Chu, N. Ru, L. Perfetti, D. H. Lu, M. Wolf, I. R. Fisher, and Z.-X. Shen, Science **321**, 1649 (2008).

[3] P. Beaud, A. Caviezel, S. O. Mariager, L. Rettig, G. Ingold, C. Dornes, S.-W. Huang, J. A. Johnson, M. Radovic, T. Huber, T. Kubacka, A. Ferrer, H. T. Lemke, M. Chollet, D. Zhu, J. M. Glownia, M. Sikorski, A. Robert, H. Wadati, M. Nakamura, M. Kawasaki, Y. Tokura, S. L. Johnson, and U. Staub, Nat. Mater. **13**, 923 (2014).

[4] S. Wall, D. Wegkamp, L. Foglia, K. Appavoo, J. Nag, R. Haglund, J. Stähler, and M. Wolf, Nat. Commun. **3**, 721 (2012).

[5] D. Emin and T. Holstein, Phys. Rev. Lett. **36**, 323 (1976).

[6] R. Peierls, *Quantum Theory of Solids* (Oxford University Press, Oxford, UK, 1955).

[7] R. J. H. Clark, M. Kurmoo, D. N. Mountney, and H. Toftlund, J. Chem. Soc., Dalton Trans. **1851** (1982).

[8] S. Dexheimer, A. V. Pelt, J. Brozik, and B. Swanson, Synth. Met. **116**, 393 (2001).

[9] K. Toriumi, M. Yamashita, S. Kurita, I. Murase, and T. Ito, Acta Crystallogr. Sect. B **49**, 497 (1993).

[10] T. Suemoto, H. Nakao, M. Nakajima, and H. Kitagawa, J. Chem. Phys. **134**, 224503 (2011).

[11] F. X. Morrissey, J. G. Mance, A. D. V. Pelt, and S. L. Dexheimer, J. Phys.: Condens. Matter **25**, 144204 (2013).

[12] R. J. H. Clark and M. Kurmoo, J. Chem. Soc., Dalton Trans. **524** (1981).

[13] S. Takaishi and M. Yamashita, Philos. Trans. R. Soc. London A **366**, 93 (2008).

[14] B. Scott, B. L. Bracewell, S. R. Johnson, B. I. Swanson, J. F. Bardeau, A. Bulou, and B. Hennion, Chem. Mater. **8**, 321 (1996).

[15] Y. Wada, T. Mitani, M. Yamashita, and T. Koda, J. Phys. Soc. Jpn. **54**, 3143 (1985).

[16] J. T. Gammel, A. Saxena, I. Batistić, A. R. Bishop, and S. R. Phillpot, Phys. Rev. B **45**, 6408 (1992).

[17] T. Suemoto, Y. Takahashi, K. Yasukawa, D. Kawakami, S. Takaishi, M. Yamashita, A. Kobayashi, and H. Kitagawa, J. Lumin. **128**, 1081 (2008).

[18] S. M. Weber-Milbrodt, J. T. Gammel, A. R. Bishop, and E. Y. Loh, Phys. Rev. B **45**, 6435 (1992).

[19] F. X. Morrissey and S. L. Dexheimer, J. Phys. Chem. B **116**, 10582 (2012).

[20] T. Suemoto and S. Tomimoto, J. Lumin. **83–84**, 13 (1999).

[21] H. Okamoto, Y. Oka, T. Mitani, and M. Yamashita, Phys. Rev. B **55**, 6330 (1997).

[22] S. Tomimoto, S. Saito, T. Suemoto, K. Sakata, J. Takeda, and S. Kurita, Phys. Rev. B **60**, 7961 (1999).

[23] A. Sugita, T. Saito, H. Kano, M. Yamashita, and T. Kobayashi, Phys. Rev. Lett. **86**, 2158 (2001).

[24] S. Tomimoto, S. Saito, T. Suemoto, J. Takeda, and S. Kurita, Phys. Rev. B **66**, 155112 (2002).

[25] K. Kimura, H. Matsuzaki, S. Takaishi, M. Yamashita, and H. Okamoto, Phys. Rev. B **79**, 075116 (2009).

[26] P. R. Poulin and K. A. Nelson, Science **313**, 1756 (2006).

[27] T. Shin, J. W. Wolfson, S. W. Teitelbaum, M. Kandyla, and K. A. Nelson, Rev. Sci. Instrum. **85**, 083115 (2014).

[28] K. Sigeo, Bull. Chem. Soc. Jpn. **38**, 1804 (1965).

[29] M. Naohide, Y. Masahiro, and K. Sigeo, Bull. Chem. Soc. Jpn. **51**, 2334 (1978).